PLASMID CARRIAGE AND THE UNORTHODOX USE OF FISHER'S THEOREM IN EVOLUTIONARY BIOLOGY

CARLOS REDING[1,2*]

[1]*Department of Genetics, Stanford University. Stanford, CA 94305, USA.*
[2]*Faculty of Life Sciences, University of Bristol. BS2 8BH Bristol, United Kingdom.*

[*]**Corresponding author:** rc_reding@teknik.io

The link between fitness and reproduction rate is a central tenet in evolutionary biology: mutants reproducing faster than the dominant wild-type are favoured by selection, otherwise the mutation is lost. This link is given by Fisher's theorem under the assumption that fitness can only change through mutations. Here I show that fitness, as formalised by Fisher, changes through time without invoking new mutations—allowing the co-maintenance of fast- and slow-growing genotypes. The theorem does not account for changes in population growth that naturally occur due to resource depletion, but it is key to this unforeseen co-maintenance of growth strategies. To demonstrate that fitness is not constant, as Fisher's theorem predicates, I co-maintained a construct of *Escherichia coli* harbouring pGW155B, a non-transmissible plasmid that protects against tetracycline, in competition assays without using antibiotics. Despite growing 40% slower than its drug-sensitive counterpart, the construct with pGW155B persisted throughout the competition without tetracycline—maintaining the plasmid. Thus, predicting the selection of microbial genotypes may be more difficult than previously thought.

I. INTRODUCTION

Textbook population genetics [1–3] and textbook microbiology [4] define the fitness of microbial populations as the intrinsic population growth rate. This notion stems from Fisher's theorem of natural selection [5] where fitness (m) is given by the exponential model $N(t) = N_0 e^{mt}$. Here N_0 is the initial number of individuals of a given genotype, and $N(t)$ the number of individuals at time t. Thus, the ratio $W_{ij} = m_i/m_j$ gives the fitness of a mutant with respect to another (W_{ij}). Given the simplicity of Fisher's theorem, it is widely used to study microbial evolution [6–10] and measure the fitness of microbial genotypes through fitness competition assays [6, 11–14]. If fitness is exclusively given by population growth rate, and it is an inherited trait, it is reasonable to expect that mutants with greater fitness will be represented with greater proportion in the next generation thereby replacing the wild-type genotype [1, 5].

However, slow growth strategies abound among microbes [15–18]. The ubiquity of plasmids, for example, cannot be explained with this paradigm given the reduction in fitness they impose [19–21]. This discrepancy can be explained by analysing Fisher's theorem. Fisher assumes that m_i/m_j is constant, consistently with the view that fitness is inheritable and therefore it can only change through mutations that affect m [6]. Below I show it is not, exposing conditions where slow reproducing genotypes can be maintained through time when competing against genotypes that reproduce faster. Even in the absence of trade-offs between reproduction and survival [22]. Relying on my new analysis of Fisher's theorem, I co-maintained a construct of *Escherichia coli* harbouring a non-transmissible plasmid, with a tetracycline resistance gene, in fitness competition assays without using antibiotics. The plasmid imposed a 40% reduction in growth rate with respect to its plasmid-free counterpart, but the bacterium kept it even without tetracycline. This, in turns, suggests that selection for plasmids, commonly studied through Fisher's theorem, may be stronger than previously thought—explaining their ubiquity in nature.

II. Results

Let me assume two competing genotypes, mutants A and B, that grow consistently with population genetics theory [1, 2]. The following system of ordinary differential equations describes the change in the number of individuals of each mutant over time:

$$\frac{dA}{dt} = m_a A, \quad \frac{dB}{dt} = m_b B, \tag{1}$$

where m is the population growth rate increase as introduced above, and $A(0) = B(0) = x$ where x is strictly positive. Note that m is derived from random birth (b) and death (d) rates, so that $m = b - d$ [1], and that it is independent of the number of individuals of each genotype. Each individual is equally likely to die or reproduce at any given time, and the age distribution is near to the equilibrium so that b and d are nearly constant. The growth dynamics of both mutants is illustrated in Figure 1A. If b and d are constant, m is a constant and therefore the relative fitness difference between genotypes $W_{ba} = m_b/m_a = k$ is also constant. In other words, if $m_b = \frac{ln[B(t)/B(0)]}{t}$ as derived from the exponential model introduced above [2, 6, 23], and $B(t)$ is the number of individuals of mutant B at an arbitrary time t, the relative fitness W_{ba} is the same regardless of t. The same applies to the fitness of A with respect to B. Indeed, if $m_b > m_a$, the number of mutant B individuals is higher than those of mutant A at all times as Figure 1A shows.

Now suppose that m depends on the number of individuals of each genotype. This is a reasonable assumption given that resources are depleted during microbial growth, and

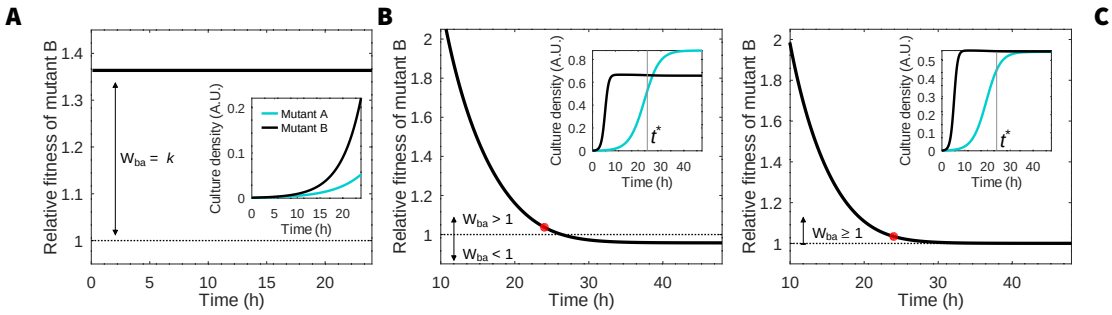

Figure 1. Change in relative fitness when populations have exponential and logistic growth. A) Change in relative fitness of mutant B (W_{ba}, black) over time when competing mutants have density-independent, exponential growth—assumed by population genetics theory for populations with continuous growth and overlapping generations [1, 2]. Relative fitness was calculated as [6] $W_{ba} = m_b/m_a$, where m corresponds to the population growth rate for each mutant. The fitness of mutant A, reference, is shown as a black, dotted line. The inset shows the change in cell density, in arbitrary units (A. U.), during the competition. **B-C)** The same information is shown for mutants with density-dependent growth, with (B) and without (C) trade-off between reproduction rate and survival. The sampling time $t^* = 24$ hours, commonly used in microbiological assays, is noted by a red marker in the main plot, and a vertical, grey line in the insets.

that resources are finite, limiting the abundance of each mutant over time:

$$\frac{dA}{dt} = m_a\left(1 - \frac{A}{K_a}\right)A, \quad \frac{dB}{dt} = m_b\left(1 - \frac{B}{K_b}\right)B. \tag{2}$$

Here K_a and K_b are the maximal population size attainable (*carrying capacity*) for mutants A and B, respectively, resulting from the limited availability of resources. Now, the population growth rate m is corrected by the term $1 - (N_i/K_i)$. The Lotka-Volterra model of competition [24] includes the term $1 - (N_i - \alpha_{ij}N_j)/K_i$, where $\alpha_{ij}N_j$ is the linear reduction in growth rate—in terms of K—of species i by competing species j. But for simplicity I assumed the interference between species is negligible and therefore $\alpha_{ij}N_j \approx 0$. This formalisation describes the limitation in growth imposed by the environment, due to finite resources, reducing m and the growth of both genotypes over time (Figure 1B and C). In this scenario, m_b depends on the carrying capacity of mutant B *and* mutant A, with the relative fitness changing to

$$W_{ba} = \frac{m_b\left[1 - \left(B/K_b\right)\right]}{m_a\left[1 - \left(A/K_a\right)\right]} = \frac{m_b^*}{m_a^*}. \tag{3}$$

In other words, W_{ba} will change through time until both mutants reach their carrying capacities, and W_{ba} becomes the ratio of carrying capacities so $W_{ab} = K_b/K_a = k$ is constant. Only after this point fitness can be measured with no variation though time. Curiously, in this scenario m is still calculated as $m_b = \frac{ln[B(t)/B(0)]}{t}$ [6, 11–14]. Estimating

fitness differences between two genotypes using equation (3), however, requires prior knowledge of the carrying capacity which can be problematic [6].

The result when m_b is calculated in biological populations, where their growth is limited by resource availability, is illustrated in Figures 1B and C: fitness declines exponentially over time, and whether a mutant is more or less fit that the reference genotype will be given by the choice of t, an arbitrary perior during which genotypes are allowed to grow, and therefore $B(t)$. Thus, depending on the combination of carrying capacities, rates of population increase, and sampling time, a mutant may be fitter, as fit, or less fit than the reference genotype.

If, say, $m_b > m_a$ and $W_{ba} > 1$, which mutant, A or B, would be selected in pairwise competition assays? Despite the simplicity of equations (1) and (2), the answer is not straightforward. Figure 2 illustrates the change in relative abundance of two genotypes, A, and B, growing in competition for a common resource. These genotypes are haploid, with continuous growth and overlapping generations where m_a and m_b represent their population growth rates as introduced above. The competition is propagated at regular intervals c where the new initial conditions are given by $N_a(c_{+1}, 0) = N_a(c, t^*)d$, $N_b(c_{+1}, 0) = N_b(c, t^*)d$, with t^* being the time of growth allowed prior to the propagation and $0 \leq d \leq 1$ the dilution factor during the propagation step analog to experimental assays [6, 7, 13]. Following population genetics theory [1, 3, 4, 6], the outcome of this competition if straightforward: if, say, mutant B reproduces faster than mutant A ($m_b > m_a$), then $W_{ab} = m_a/m_b < 1$ and mutant A goes extinct (Figure 2A). Regardless of how long the competition is allowed to progress until the next propagation step, mutant A is always lost in competition with B. Only through the emergence of a new mutant A* with $m_a^* > m_b > m_a$ should this prediction change.

But when fitness changes through time the outcome of the competition becomes unclear, now depending on whether the competing genotypes reach their carrying capacities before the propagation: if the competition is propagated very frequently, so that *both* genotypes are in active growth, the genotype reproducing faster will replace that reproducing slower consistently with Fisher's theorem. However, if one or both genotypes are allowed to reach their carrying capacities, both will be be co-maintained regardless of the in rates of population increase (Figures 2B and C). Here the relative frequency will be given by their carrying capacities K, so if reproduction and carrying capacity engage in a trade-off [22] for one genotype, this will be most frequent (Figure 2B).

To test this prediction, I competed two constructs of *Escherichia coli* MC4100, Wyl and GB(c) (see Methods), and measured their variation in fitness through time. Figure 3A shows that both constructs reach their carrying capacicies within 24 hours. The construct GB(c) carries the non-transmissible plasmid pGW155B [25] harbouring *tet(36)*—a

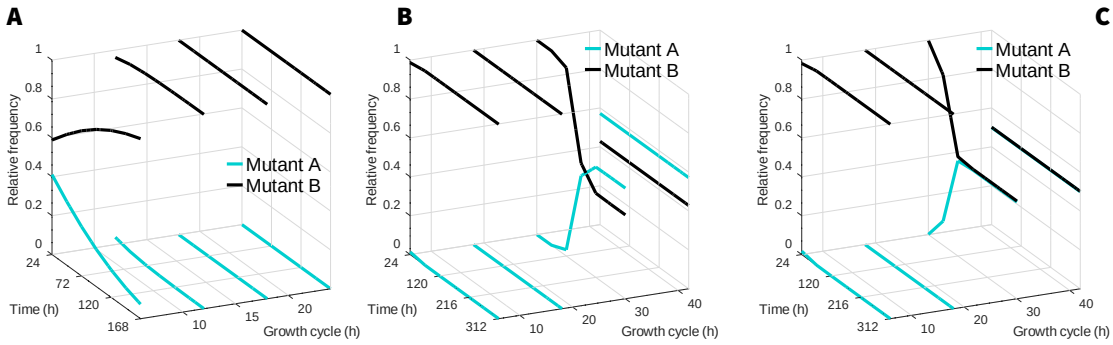

Figure 2. Change in relative frequency during competition depending on the length of the growth cycle. Changes in frequency over time for mutants A (cyan) and B (black) following propagations at arbitrary times t=6h, t=12h, t=18h, and t=24h. These times correspond to different stages of growth as Figure 1 shows. Each plot illustrate the case for genotypes with density-independent growth (A), or density-dependent growth where a genotype does not engage in a trade-off between reproduction and survival (B) and when it does not (C).

ribosome-protection type resistance gene against tetracycline [25]. This plasmid lacks a *rep* gene to control tightly the partition of plasmids after cell division [26–28] (addgene vector database accession #2853). While pGW155B is a synthetic plasmid, many natural plasmids also lack partition systems [28, 29]. Both constructs have identical chromosome with exception of this plasmid, and the fluorescence gene they carry: cyan (*cfp*, GB(c)) or yellow (*yfp*, Wyl), to allow their identification in competition assays. Using a non-transmissible plasmid prevents cross-contamination by horizontal gene transfer between the resistant construct GB(c) and Wyl. Importantly, the use of constructs derived from MC4100 avoids interactions between competitors that may affect the outcome of the competition for reasons beyond pGW155B, like the production of bacteriocins [30].

pGW155B penalised the population growth rate of construct GB(c) by approximately 40% compared to Wyl (Figure 3B) as I found out using pure cultures. The duration of lag, and carrying capacity were also sensitive to plasmid carriage, regardless of whether I measured the growth using fluorescence or light scattering (Figure S1). Changes in cell size could confound optical density and fluorescence readings, but this phenomenon leaves a signature [31] in growth data that is absent in my dataset (Figures S1, S2, and S3). The change in carrying capacity K can be linked to an increase in biomass yield (y) as Monod's expression [32] $y = K/S$ suggests, where S the supply of glucose. This metric is consistent the data, given that construct GB(c) has to express and translate plasmid-borne genes with the same supply of glucose (Figures 3B and C). This means that pGW155B triggers a metabolic trade-off between growth rate and biomass yield redolent of rK-selection theory[22, 33].

For the competition assay, I mixed equal proportions (cell/cell) of two pure cultures,

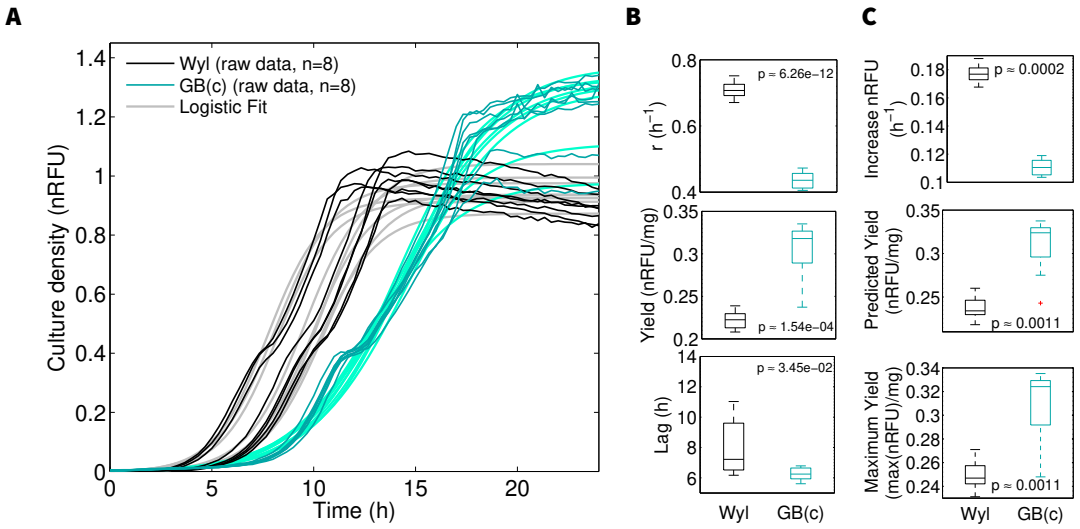

Figure 3. Asymmetric carriage costs of pGW155B. A) Overlapped growth curves of constructs Wyl (black) and GB(c) (cyan) in the absence of tetracycline over 24h. I estimated the maximum growth rate (r), population size in the equilibrium (K), biomass yield, and lag duration from a 4-parameter logistic model fitted to growth data (see Methods). Data fits for constructs Wyl and GB(c) are shown in grey and light cyan, respectively. **B)** Box plots showing the median (centre of the box), 25th and 75th percentile for each of the aforementioned parameters. The whiskers extend to the most extreme data points that are not outliers, and these are individually represented. The p value shown refers to a Two-sample t-test with unequal variance (8 replicates) that I used to test differences in the parameters between both constructs. **C)** Alternative metrics for growth rate and biomass yield: forward Euler approximation (top), data fit predicted yield (middle), and maximal yield across all time points in growth data (bottom). The p values correspond to Two-sample t-tests with unequal variance (8 replicates).

from construct GB(c) and Wyl respectively, grown overnight, in media containing no antibiotic or 0.04 µg/mL of tetracycline (see Methods). I incubated the mixed culture at 30^{o}C until both constructs reached their carrying capacity (K, $\sim$ 24h as per data in Figure 3A), and then I propagated the competition into a new plate containing fresh media. I repeated the propagation step seven times totalling between 77 (GB(c)) and 119 (Wyl) generations. Indeed, the relative fitness of both constructs changed through time. In the presence of tetracycline the relative fitness of drug-sensitive construct Wyl was below GB(c), which harbours pGW155B, at all times as Figure 4A illustrates. This meant that GB(c) increased its relative frequency in following propagation steps and became the most abundant construct throughout the competition (Figure 4B). During the competition, the number of copies of pGW155B harboured by GB(c) increased 5- to 6-fold driven by exposure to tetracycline (2-sample t-test with unequal variances, p=0.0088, df=2.5826, t-statistic=-7.2441; with 3 replicates. Figure 4C) as it would be reasonable to expect given the exposure to tetracycline. However, Wyl never goes extinct consistently with Figure 2—note the model does not implement mutations events likely to occur in

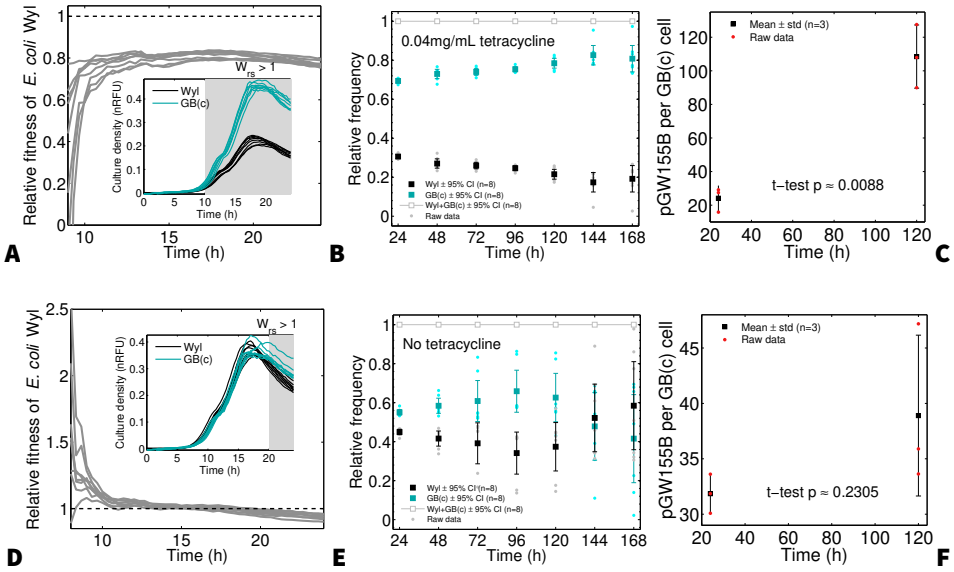

Figure 4. Time-dependent fitness data allows co-maintenance of both constructs without tetracycline. Relative fitness during first 24 hour pairwise-competition of construct Wyl, where both constructs grew in media supplemented with 0.04 µg/mL of tetracycline (**A**) and without drug (**D**). Fitness for each replicate is presented with respect to the reference GB(c) (black dashed line). The inset illustrate the growth curves for both constructs, highlighting in grey the period where the relative fitness of Wyl (W_{sr}) is lower than its tetracycline-resistant competitor's. **B)** and **E)** show the change in relative frequency of both constructs through time when both constructs grew in media supplemented with tetracycline (B) and without antibiotic (E). Error bars represent the mean ± 95% confidence intervals, with raw data points shown as dots. **C)** and **F)** show the change in relative copy numbers of pGW155B borne by construct GB(c) during the pairwise-competition, calculated using quantitative PCR (see Methods). Error bars represent the mean ± standard deviation, with raw data shown in red.

vitro.

Similarly, when both constructs grew in mixed cultures without tetracycline exposure, the relative fitness of Wyl can be higher, equal, or lower than construct GB(c) through time as Figure 4D shows. This meant that both constructs where co-maintained, and with similar relative frequencies, despite the difference in growth rate (Figure 4E). In other words, pGW155B persisted despite the lack of tetracycline and the difference in growth rates with no substantial variation in the number of plasmids harboured per cell (2-sample *t*-test with unequal variances, p=0.2305, df=2.2351, t-statistic=-1.6353; with 3 replicates. Figure 4F). This contrasts with previous studies [13] showing the rapid decline, within a similar time frame, in bacteria harbouring non-transmissible plasmids.

III. Discussion

Experimentalists rely extensively on Fisher's theorem to study whether mutations are beneficial or deleterious. The misconception in Fisher's theorem highlighted in this study is mathematically simple, but the result contests a basic tenet in evolutionary biology: reproduction is not all that matters. Indeed, data show that prokaryotes that slow grow are just as abundant as those growing substantially faster [18, 34]. This is what predictions in Figures 2B and C suggest. If the frequency of selection is low, caused for example by long periods of extreme starvation [35, 36], slow- and fast-growing genotypes can be co-maintained. This is particularly relevant to understand the abundance of plasmids, difficult to understand Fisher's rationale [21].

It is noteworthy to separate the phenomenon described in this manuscript from rK-selection theory [33]. This theory postulates that selection cannot simultaneously optimise the growth rate and population size and therefore that they engage in a trade-off. Here I postulate that fitness shifts from reproduction to carrying capacity as populations grow, not necessarily in evolutionary timescales. Thus, when selection occurs will determine whether fast- or slow-growing will be favoured. Thus, while pGW155B indeed triggers a trade-off redolent of rK-selection, the theoretical predictions Figures 1C and 2C as well as the data highlight that rK trade-offs have no effect on the predicted co-existence of competing genotypes. In this new light, for example, the costs of plasmid carriage become relative of the frequency of selection. Conditions of high frequency, say, caused by repeated exposure to antibiotics during therapies, could indeed favour genotypes with higher growth rates. But the rationale needs not apply when selection is less frequent, where both growth strategies can be co-maintained—explaining the abundance of plasmids in nature despite the growth penalty they impose on their hosts.

IV. Methods

Media and Strains. I used the strains of *Escherichia coli* GB(c) and Wyl [37] (a gift from Remy Chait and Roy Kishony), and M9 minimal media supplemented with 0.4% glucose and 0.1% casamino acids (w/v). I made tetracycline stock solutions from powder stock (Duchefa, Ref. #0150.0025) at 5mg/mL in 50% ethanol, filter sterilised, and stored at -20^oC. Subsequent dilutions were made from this stock in supplemented M9 minimal media and kept at 4^oC.

Batch transfer protocol. I inoculated a 96-well microtitre plate containing 150 µg/mL of supplemented M9 media with a mixture of two overnight cultures, one of *E. coli* GB(c)

and another of *E. coli* Wyl (1µL containing approx. $2 \cdot 10^8$ cells, Figure S2). The overnight culture for GB(c) was supplemented with 100ng/mL of tetracycline to preserve the plasmid pGW155B carrying *tet(36)* as described elsewhere [7], then centrifuged and removed prior adding to the microtitre plate. I incubated the plate at 30^{o}C in a commercial spectrophotometer and measured the optical density of each well at 600nm (OD_{600}), yellow florescence for the Wyl strain (YFP excitation at 505nm, emission at 540nm), and cyan fluorescence for the GB(c) strain (CFP at 430nm/480nm) every 20min for 24h. After each day I transferred 1.5µL of each well, using a 96-well pin replicator, into a new microtitre plate containing fresh growth medium and tetracycline.

Growth parameter estimation. Yellow and cyan fluorescence protein genes were constitutively expressed given the constant ratio between fluorescence and optical density (Figure S4). This allowed me to use fluorescence data as a proxy for cell density in mixed culture conditions. I normalised fluorescence readings using a conversion factor, n_f, calculated by growing each construct in a range of glucose concentrations, and regressing the linear model RFU = $n_{\mathrm{f}} \cdot$ OD + c, where RFU is relative fluorescence units data, OD optical density data, n_f the conversion factor between fluorescence and optical density, and c the crossing point with the y–axis when OD = 0. I imported the resulting time series data set (Figures S3) into `MATLAB R2014b` to subtract background and calculate fitness as described in the main text.

DNA material extraction. For each concentration, I sampled three representative 150 µg/mL replicates that I divided in two groups: for chromosome and plasmid DNA extraction. I used 'GeneJet DNA' (ThermoScientific, Ref. #K0729) and 'GeneJet Plasmid' (ThermoScientific, Ref. #K0502) extraction kits to extract chromosomal and plasmid DNA (pDNA) from the samples, respectively, and used Qubit to quantify DNA and pDNA yields. Both extracts were diluted accordingly in extraction buffer, as per in manufacturer instructions, to normalise DNA across samples.

Quantitative PCR and plasmid copy number estimation. I used `primer3` to design two pairs of primers with melting temperature (T_m) of 60^{o}C and non-overlapping probes with T_m of 70^{o}C. The amplicon ranges between 100 to 141bp depending on the locus (Table 1). Two reaction mixes were prepared using the kit 'Luminaris Color Probe Low ROX' (ThermoScientific, Ref. #K0342), adding 0.3µM of each primer and 0.2µM of the probe as per manufacturer specifications. Following a calibration curve for each reaction (Figure S5) I added 0.01ng of chromosomal or plasmid DNA material to each of the reaction mixes.

Table 1. Primers and probes designed using `Primer3`. Amplicon ranging from 100 to 141bp. T_m indicates the estimated melting temperature.

Target gen	Sequence ($5' \rightarrow 3'$)	T_m (^{o}C)	Feature
tatB	CGATGAAGCGTTCCTACGTT	60.27	Forward
	TCATGCGCAGCTTCATTATC	59.94	Reverse
	AAGGCGAGCGATGAAGCGCA	70.70	Probe
tet(36)	ATTGGGCATCTATTGGCTTG	59.22	Forward
	CCGATTCACAGGCTTTCTTG	60.76	Reverse
	AGCCTTTGCCAATTGGGGCG	70.37	Probe

To estimate the relative copies of pGW155B per GB(c) cell, I calculated the corresponding proportion of chromosomal DNA corresponding to the GB(c)-type from data in Figure 4 and used the expression [13]

$$cn = \frac{(1+E_c)^{Ctc}}{(1+E_p)^{Ctp}} \times \frac{S_c}{S_p},$$

where cn is the number of plasmid copies per chromosome, S_c and S_p are the size of the chromosome and pGW155B amplicon in bp, E_c and E_p the efficiency of the qPCR taken from data in Figure S5, and Ctc and Ctp are the cycles at which I first detected product amplification (C_t).

REFERENCES

1. Crow, J. F., Kimura, M., *et al. An introduction to population genetics theory.* (New York, Evanston and London: Harper & Row, Publishers, 1970).
2. Nagylaki, T. in *Introduction to Theoretical Population Genetics* 5–27 (Springer, 1992).
3. Templeton, A. *Population Genetics and Microevolutionary Theory* ISBN: 9780471409519 (Wiley, 2006).
4. Dawes, I. & Sutherland, I. *Microbial Physiology* ISBN: 9780632024636 (Wiley, 1992).
5. Fisher, R. A. *The Genetical Theory of Natural Selection* 308–315 (At The Clarendon Press, 1930).
6. Lenski, R. E., Rose, M. R., Simpson, S. C. & Tadler, S. C. Long-Term Experimental Evolution in Escherichia coli. I. Adaptation and Divergence During 2,000 Generations. *Am. Nat.* **138,** pp. 1315–1341 (1991).

7. Chait, R., Craney, A & Kishony, R. Antibiotic interactions that select against resistance. *Nature* **446,** 668–671 (2007).

8. Wang, H., Avican, K., Fahlgren, A., *et al.* Increased plasmid copy number is essential for Yersinia T3SS function and virulence. *Science* **353,** 492–495 (2016).

9. Adkar, B. V., Manhart, M., Bhattacharyya, S., Tian, J., Musharbash, M. & Shakhnovich, E. I. Optimization of lag phase shapes the evolution of a bacterial enzyme. *Nat. Ecol. Evol.* **1,** 1–6 (2017).

10. Concepción-Acevedo, J., Weiss, H. N., Chaudhry, W. N. & Levin, B. R. Malthusian parameters as estimators of the fitness of microbes: a cautionary tale about the low side of high throughput. *PLoS One* **10,** e0126915 (2015).

11. Andersson, D. I. & Levin, B. R. The biological cost of antibiotic resistance. *Curr. Opin. Microbiol.* **2,** 489–493 (1999).

12. Gullberg, E., Cao, S., Berg, O. G., *et al.* Selection of resistant bacteria at very low antibiotic concentrations. *PLoS Pathog.* **7,** e1002158 (July 2011).

13. Millán, A. S., Peña-Miller, R., Toll-Riera, M, *et al.* Positive selection and compensatory adaptation interact to stabilize non-transmissible plasmids. *Nat. Commun.* **5** (2014).

14. Ram, Y., Dellus-Gur, E., Bibi, M., *et al.* Predicting microbial growth in a mixed culture from growth curve data. *Proc. Natl. Acad. Sci. U.S.A.* **116,** 14698–14707 (2019).

15. Kussell, E., Kishony, R., Balaban, N. Q. & Leibler, S. Bacterial persistence: a model of survival in changing environments. *Genetics* **169,** 1807–1814 (2005).

16. Pedrós-Alió, C. Marine microbial diversity: can it be determined? *Trends Microbiol.* **14,** 257–263 (2006).

17. Lever, M. A., Rogers, K. L., Lloyd, K. G., *et al.* Life under extreme energy limitation: a synthesis of laboratory-and field-based investigations. *FEMS Microbiol. Revs.* **39,** 688–728 (2015).

18. Flemming, H.-C. & Wuertz, S. Bacteria and archaea on Earth and their abundance in biofilms. *Nat. Rev. Microbiol.* **17,** 247–260 (2019).

19. Smillie, C., Garcillán-Barcia, M. P., Francia, M. V., Rocha, E. P. & de la Cruz, F. Mobility of plasmids. *Microbiol. Mol. Biol. Rev.* **74,** 434–452 (2010).

20. Harrison, E. & Brockhurst, M. A. Plasmid-mediated horizontal gene transfer is a coevolutionary process. *Trends Microbiol.* **20,** 262–267 (2012).

21. Probing the plasmid paradox. *Nat. Ecol. Evol.* **5,** 1559–1559 (2021).

22. Reding-Roman, C., Hewlett, M., Duxbury, S., Gori, F., Gudelj, I. & Beardmore, R. The unconstrained evolution of fast and efficient antibiotic-resistant bacterial genomes. *Nat. Ecol. Evol.* **1,** 0050 (2017).

23. Hansen, S. K., Rainey, P. B., Haagensen, J. A. & Molin, S. Evolution of species interactions in a biofilm community. *Nature* **445,** 533–536 (2007).

24. Gilpin, M. E. & Ayala, F. J. Global models of growth and competition. *Proc. Natl. Acad. Sci. U.S.A.* **70,** 3590–3593 (1973).

25. Whittle, G, Whitehead, T. R., Hamburger, N, Shoemaker, N. B., Cotta, M. A., *et al.* Identification of a new ribosomal protection type of tetracycline resistance gene, tet(36), from swine manure pits. *Appl. Environ. Microbiol.* **64,** 4151–4158 (2003).

26. Del Solar, G. & Espinosa, M. Plasmid copy number control: an ever-growing story. *Mol. Microbiol* **37,** 492–500 (2000).

27. Garcillán-Barcia, M. P., Alvarado, A. & de la Cruz, F. Identification of bacterial plasmids based on mobility and plasmid population biology. *FEMS Microbiol. Rev.* **35,** 936–956 (2011).

28. Million-Weaver, S. & Camps, M. Mechanisms of plasmid segregation: have multicopy plasmids been overlooked? *Plasmid* **75,** 27–36 (2014).

29. Guynet, C. & de la Cruz, F. Plasmid segregation without partition. *Mob. Genet. Elements* **1,** 236–241 (2011).

30. Dobson, A., Cotter, P. D., Ross, R. P. & Hill, C. Bacteriocin Production: a Probiotic Trait? *Appl. Environ. Microbiol.* **78,** 1–6 (2012).

31. Stevenson, K., McVey, A. F., Clark, I. B., Swain, P. S. & Pilizota, T. General calibration of microbial growth in microplate readers. *Sci. Rep.* **6,** 1–7 (2016).

32. Monod, J. *Recherches sur la croissance des cultures bactériennes* PhD thesis (Paris, 1941).

33. Reznick, D., Bryant, M. J. & Bashey, F. r-and K-selection revisited: the role of population regulation in life-history evolution. *Ecology* **83,** 1509–1520 (2002).

34. Ernebjerg, M. & Kishony, R. Distinct growth strategies of soil bacteria as revealed by large-scale colony tracking. *Appl. Environ. Microbiol.* **78,** 1345–1352 (2012).

35. Gray, D. A., Dugar, G., Gamba, P., Strahl, H., Jonker, M. J. & Hamoen, L. W. Extreme slow growth as alternative strategy to survive deep starvation in bacteria. *Nat. Commun.* **10,** 1–12 (2019).

363 36. Shoemaker, W. R., Jones, S. E., Muscarella, M. E., Behringer, M. G., Lehmkuhl,
364 B. K. & Lennon, J. T. Microbial population dynamics and evolutionary outcomes
365 under extreme energy limitation. *Proc. Natl. Acad. Sci. U.S.A.* **118,** e2101691118
366 (2021).

367 37. Chait, R., Shrestha, S., Shah, A. K., Michel, J.-B. & Kishony, R. A Differential
368 Drug Screen for Compounds That Select Against Antibiotic Resistance. *PLoS One*
369 **5,** e15179 (2010).

370 **Competing interests.** The author declares no competing interests.

371 **Acknowledgements.** The author thanks Robert Beardmore for laboratory support in the
372 early states of this study.

I. Supplementary Figures

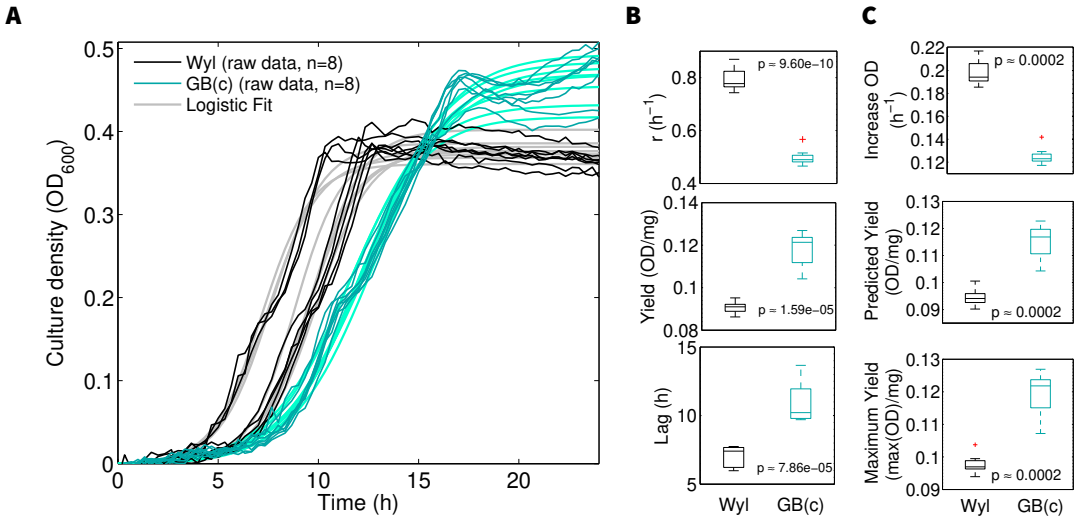

Figure S1. Asymmetric carriage costs of pGW155B (optical density data). A) Overlapped growth curves of constructs Wyl (black) and GB(c) (cyan) in the absence of tetracycline over 24h. I estimated the maximum growth rate (r), population size in the equilibrium (K), biomass yield, and lag duration from a 4-parameter logistic model fitted to growth data (see Methods). Data fits for constructs Wyl and GB(c) are shown in grey and light cyan, respectively. **B)** Box plots showing the median (centre of the box), 25th and 75th percentile for each of the aforementioned parameters. The whiskers extend to the most extreme data points that are not outliers, and these are individually represented. The p value shown refers to Two-sample t-tests with unequal variance (8 replicates) that I used to test differences in the parameters between both constructs. **C)** Alternative metrics for growth rate and biomass yield: forward Euler approximation (top), data fit predicted yield (middle), and maximal yield across all time points (bottom). The p values correspond to Two-sample t-tests with unequal variance (8 replicates).

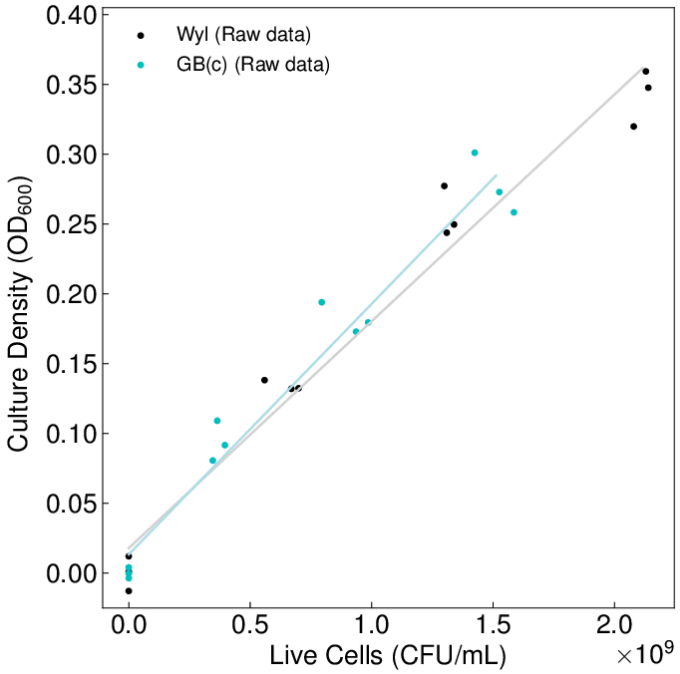

Figure S2. Calibration curve to translate optical density data to number of *Escherichia coli* cells. I fitted the linear model $a = bx + c$ to optical density and colony counting data (dots) to calculate the number of optical density units (OD_{600}) per cell. a denotes the optical density readings measured at 600nm, c the crossing point with the $y-$axis when $x = 0$, and b the conversion factor between optical density and number of cells (x). I interpolating optical density readings to calculate the number of cells within a culture as $x = (a - c)/b$. For the strain Wyl, $b = 1.62 \times 10^{-10}\ OD \cdot mL \cdot CFU^{-1}$ and $c = 1.78 \times 10^{-2}\ OD$, whereas for GB(c) $b = 1.79 \times 10^{-10}\ OD \cdot mL \cdot CFU^{-1}$ and $c = 1.33 \times 10^{-2}\ OD$.

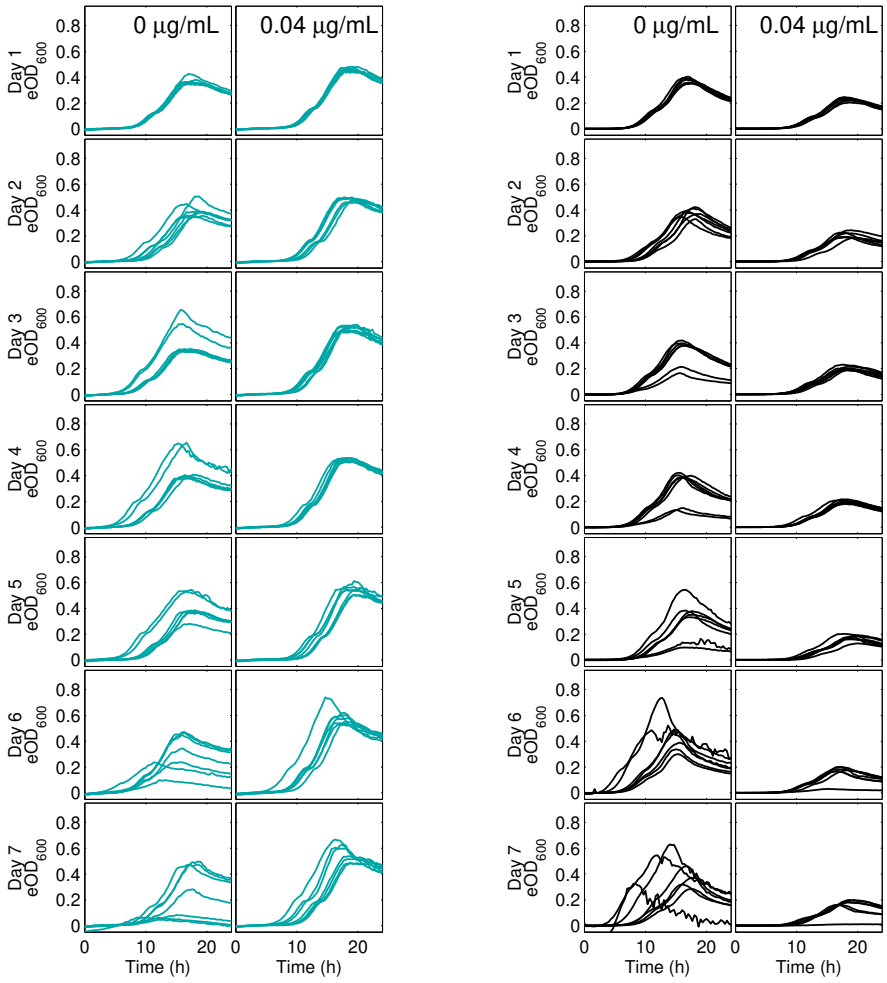

394 **Figure S3. Raw data of each construct during the competition.** Raw optical density data for GB(c) (cyan) and
395 Wyl (black), measured every 20 min and converted from fluorescence readings. Each individual plot represents
396 the change in abundance of each construct over 24 hours. Data corresponding to each condition, with and with-
397 out tetracycline, are aggregated as columns.

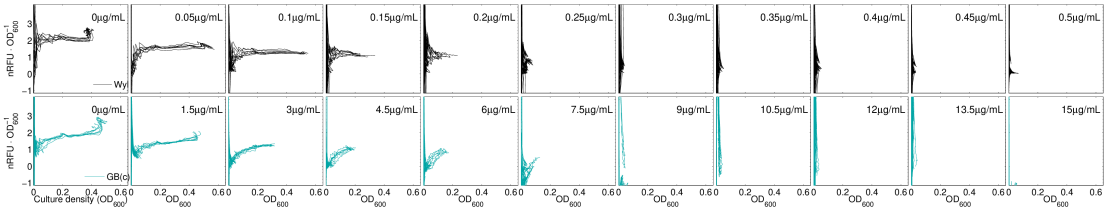

399 **Figure S4. Changes in relative fluorescence over time in GB(c) and Wyl strains in pure culture conditions.**
400 Raw change in florescence, per optical density units, measured every 20min for 24h for the Wyl- (black) and GB(c)-
401 type. Each column represents the data set for each tetracycline concentration used.

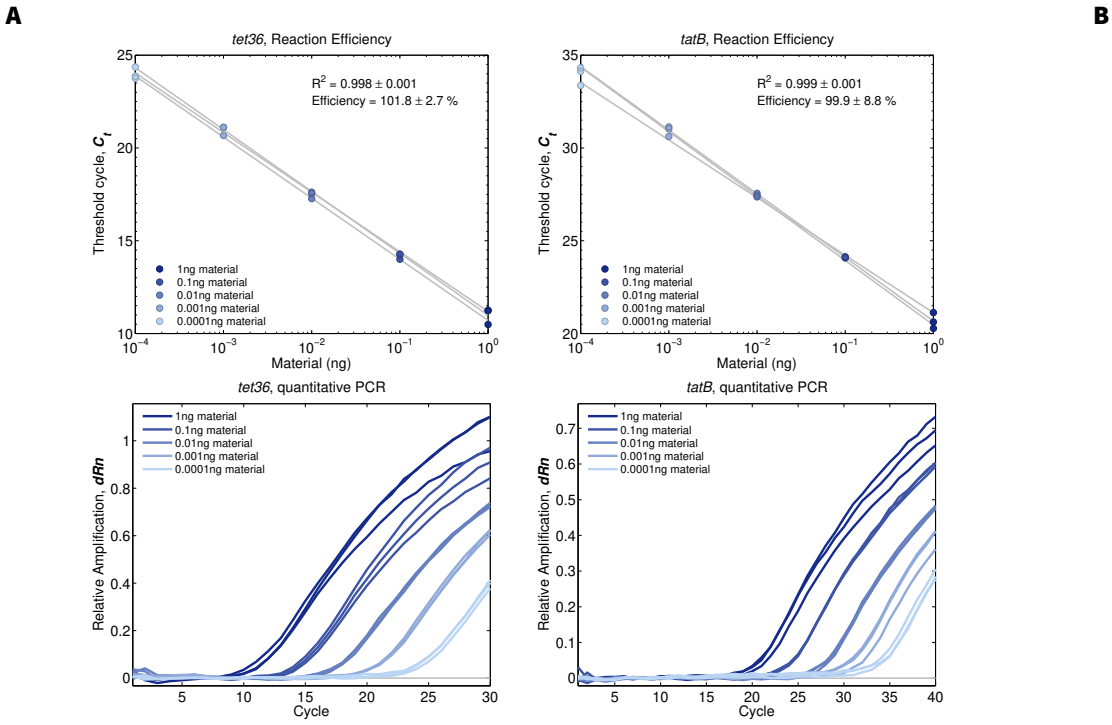

Figure S5. Quantitative PCR calibration curves for *tet(36)* and *tatB*. Reaction efficiency for the set of primers and probes, listed in Table 1 the main Methods section, for *tet(36)* (A) and *tatB*. The efficiency was calculated as $E_f = 10^{-1/Slope} - 1$, and the slope term calculated by fitting a linear model to qPCR threshold cycle (C_t) data. The mean $\pm$ standard deviation for the adjusted coefficient of determination R^2 and efficiency are shown in the figures. The amplification curves for each reaction, using 3 replicates, are shown in C) and D), respectively.